Available online at www.derpharmachemica.com

Scholars Research Library

Der Pharma Chemica, 2015, 7(11):373-383
(http://derpharmachemica.com/archive.html)

ISSN 0975-413X
CODEN (USA): PCHHAX

Inhibitive and adsorption properties of leaves extract of bitter leaf (*Vernonia amygdalina)* as corrosion inhibitor of aluminium in 1.0M NaOH

Omotioma M.[1*] and Onukwuli O. D.[2]

[1]Department of Chemical Engineering, Enugu State University of Science and Technology, Enugu, Nigeria
[2]Department of Chemical Engineering, Nnamdi Azikiwe University, Awka, Nigeria

ABSTRACT

This work examined the inhibitive and adsorption properties of leaves extract of bitter leaf (Vernonia amygdalina) as corrosion inhibitor of Al in 1M NaOH. Leaves extract of bitter leaf was characterized using Fourier transform infra-red (FT IR) spectroscopy to identify peaks of the functional groups. Weight loss, potential dynamic polarization, Fourier transform infra-red and scanning electron microscopic analyses were used for the corrosion inhibition study. The FT IR analysis of the bitter leaves extract revealed the presence of C=C-H, Ar-H (bending out of plane), C-H (bending in plane), stretched C-O, stretched C=C, stretched C=N, stretched C=O, stretched C≡C, stretched C≡N, stretched C-H and stretched O-H functional groups. Adsorption of the extract on the Al surface was spontaneous and occurred according to the mechanism of physical adsorption. The optimal conditions for the corrosion inhibition of the Al in NaOH are concentration of the inhibitor of 1.0 g/l, temperature of 303 K and immersion time of 1hr. The optimum inhibition efficiency of the bitter leaves extract is 80.54 %. Leaves extract of bitter leaf is a mixed-type inhibitor of Al in NaOH medium.

Keywords: *Corrosion inhibition, adsorption, Bitter leaf, NaOH*

INTRODUCTION

Aluminium is the third most abundant element found in nature; first two are oxygen and silicon. It is an important and widely used metal in the transport, construction, packaging and electrical sectors. Aluminium and its alloys are of economic importance because of their low cost, lightness and good corrosion resistance at moderate temperatures [1]. They are also widely used in many industries such as reaction vessels, pipes, machinery and chemical batteries because of their advantages [2]. Aluminum and its alloys are low cost and remarkable materials in industrial technology because of their light weight, high thermal and electrical conductivity as well as high resistance to corrosion in a wide variety of corrosion environments [3]. Aggressive alkaline solutions such as NaOH used for cleaning aluminium metallic structures often corrode such structures. Corrosion is the degradation of a metal by an electrochemical reaction with its environment [4]. The fundamental cause or driving force for all corrosion is the lowering of a system's Gibbs energy. The consequences of corrosion are numerous, and the effects on the safe, reliable and efficient operation of equipment or structures are often more serious than the simple loss of a mass of the metal. Failures of various kinds and the need for expensive replacements may occur even though the amount of metal destroyed is quite small. Thus, there is need for corrosion control such as application of corrosion inhibitor.

Although many studies have been carried out on suitable corrosion inhibitors, most of the inhibitors are synthetic chemicals which are very expensive and hazardous to the environment. Most of the research works do not recognize the dynamic nature of some passive films, corrosion products or deposits from other sources; nor do they even consider the possibility of a change in the surface conditions during the course of the experimental works. It is important to use natural product of plant origin as anti-corrosive agent since it is environmentally acceptable, inexpensive and readily available. The aim of this work is to examine the corrosion inhibition of aluminium in 1M

NaOH using leaves extract of bitter leaf (*Vernonia amygdalina*). *Vernonia amygdalina* popularly belongs to the family of *Asteraceae*. It is cultivated in Nigeria mainly for its nutritional value. The plant (especially the leaf) has been found useful in pharmaceutical applications [5, 6, 7].

MATERIALS AND METHODS

2.1 Extraction of the Plant Extracts
Leaves of bitter leaf were collected from Akpugo, Enugu state, Easter part of Nigeria. The leaves of the bitter leaf were sun dried for three days. The dried leaves were ground to increase the surface area and stored in a closed container. 30 grams of each of the ground plant leaves were measured and soaked in 1000ml of ethanol for 48 hours. At the end of the 48 hours, plant mixture was filtered. The filtrate obtained is a mixture of the plant extract and the ethanol. The ethanol solvent was distilled off. The concentrated plant extract was weighed and stored for the corrosion inhibition study.

2.2 Metals Preparation
The sheets of aluminium were cut into coupons (5cm x 4cm x 0.06cm). The coupons were cleaned followed by polishing with emery paper to expose shining polished surface. To remove any oil and organic impurities, the coupons were degreased with acetone and finally washed with distilled water, dried in air and then stored in desiccators. Accurate weight of each coupon was taken using electronic weighing balance and the initial weight was recorded.

2.3 Thermometric method of the Corrosion Inhibition Study
The measurements were carried using a thermostat set at 30 ^{0}C for the Aluminium in free and inhibited NaOH. The temperatures of the system containing the Aluminium and the test solution were recorded regularly until a steady temperature value was obtained. The reaction number (RN) was evaluated using Equation (1) [8, 9].

$$RN = \frac{T_m - T_i}{t} \quad (1)$$

Where T_m and T_i are the maximum and initial temperatures (in ^{0}C) respectively, and t is the time in minutes elapsed to reach T_m.

The inhibitor efficiency was determined using Equation (2) [8].

$$IE\% = 1 - \frac{RN_{add}}{RN_{free}} * 100 \quad (2)$$

Where RN_{free} and RN_{add} are the reaction numbers for the Al dissolution in free and inhibited corrosive medium respectively.

2.3 Weight Loss (Gravimetric) Method
2.3.1 Weight loss method using one factor at a time
Considering one factor at a time, the weight loss method was carried out at different temperatures and with various concentrations of the plant extracts. According to this method, weighed Al coupons were separately immersed in 250 ml open beakers containing 200 ml of 1.0M NaOH (blank). Also, Al coupons were immersed in 250 ml open beakers containing 200 ml of 1.0M NaOH with various concentrations of the plant extracts. The variation of weight loss was monitored periodically at various temperatures and in the absence and presence of various concentrations of the bitter leaves extract. At the appropriate time, the Al coupons were taken out, immersed in acetone, scrubbed with a bristle brush under running water, dried and reweighed. The weight loss (Δw), corrosion rate (CR) and inhibition efficiency (IE) were calculated using the Equations (3), (4) and (5) respectively.

$$\Delta w = w_i - w_f \quad (3)$$

$$CR = \frac{w_i - w_f}{At} \quad (4)$$

$$IE\% = \frac{\omega_0 - \omega_1}{\omega_0} * 100 \quad (5)$$

Where w_i and w_f are the initial and final weight of metal samples respectively; ω_1 and ω_0 are the weight loss values in presence and absence of inhibitor, respectively. A is the total area of the specimen and t is the immersion time. The degree of surface coverage was obtained using the following Equation (6) [10].

$$\theta = \frac{\omega_0 - \omega_1}{\omega_0} \tag{6}$$

ω_1 and ω_0 are the weight loss values in presence and absence of inhibitor.

The experimental data were used to evaluate the adsorption and thermodynamic properties. The activation energy, heat of adsorption and free energy of adsorption (ΔG_{ads}) for the corrosion inhibition were determined according to the methods used by previous works [11, 12, 13, 14, 15, 16].

2.3.2 Weight loss method using response surface method (RSM)
Response surface method in design expert software was used to design the experiment for the weight loss method. Inhibitor concentration, temperature and time were the considered factors while weight loss, corrosion rate and inhibition efficiency were the expected responses of the study. The RSM was used to analyze the responses. The ANOVA and graphical analyses of the inhibition efficiencies were carried out. The mathematical models in terms of coded and actual factors were obtained. The model in terms of coded factors was used to make predictions about the response for given levels of each factor. The high levels of the factors were coded as +1 and the low levels of the factors were coded as -1. The optimum inhibition parameters were obtained.

2.4 Potentiodynamic Polarization Study
Electrochemical test were conducted using a potentiostat/galvanostat 263 electrochemical system workstation, with a conventional three-electrode corrosion cell. A graphite rod and a saturated calomel electrode (SCE) were used as a counter and reference electrodes, respectively. Al specimen fixed in epoxy resin with a surface area of 1 cm^2 exposed to the test solution, served as the working electrode. Electrochemical measurements were carried out in aerated and unstirred solution at the end of 1800 s of immersion, which allowed the open circuit potential (OCP) to attain steady state. Temperature was fixed at 30±1 ^{0}C. Potentiodynamic polarization studies were conducted in the potential range ±250 mV versus corrosion potential at a scan rate of 0.333mV/s.

2.5 FT IR Study of the Corrosion Inhibition Process
Fourier transform infrared spectrophotometer (SHIMADZU, Model: IR affinity – 1) was used to study the functional groups of the pure bitter leaves extract, corrosion product in the presence of the bitter leaves extracts. The metals were immersed in the NaOH medium, in the presence and absence of the plant extracts. At the end of the corrosion study 30 minutes, the corrosion products in the beakers were collected with the aid of sample bottles. Comparative analysis of various FT IR produced peaks were carried out so as to determine the appropriate functional groups for the corrosion inhibition process.

2.6 Metal Surface Study using SEM Analysis
Morphological observation of the corroded Al samples were carried out using scanning electron microscopy (SEM – model: Rhenom Prox, Phenom World Eindhoven, Netherlands).

RESULTS AND DISCUSSION

3.1 Results of the Corrosion Inhibition as Determined by Thermometric Results
The effect of concentration of the bitter leaves extract (inhibitor) on the reaction number (RN) and the inhibition efficiency (IE) of the Al in the NaOH medium is presented in Table 1. Increase in concentration of the inhibitor lowers the reaction number. Also, the inhibition efficiency increases with increase in concentration of the inhibitor.

Table 1, Effect of concentration of the extract on the inhibition efficiency, IE (%)

Inhibitor conc., g/l	RN	IE (%)
0.0	0.8667	
0.2	0.4040	53.39
0.4	0.3039	64.93
0.6	0.2222	74.36
0.8	0.1464	83.11
1.0	0.1068	87.68

3.2 Experimental results of weight loss method

The experimental results of weight loss (g) and corrosion rate (mg/cm^{2}hr) using one factor at a time are presented Table 2.

Table 2 Data of corrosion inhibition of Al in NaOH with bitter leaves extract

T	Parameter	Concentration of bitter leaves extract																	
		0.0 g/l	0.2 g/l	0.4 g/l	0.6 g/l	0.8 g/l	1.0 g/l	0.0 g/l	0.2 g/l	0.4 g/l	0.6 g/l	0.8 g/l	1.0 g/l	0.0 g/l	0.2 g/l	0.4 g/l	0.6 g/l	0.8 g/l	1.0 g/l
		303 K						318 K						333 K					
t_1	Weight loss	0.29	0.17	0.13	0.11	0.1	0.09	0.36	0.23	0.177	0.16	0.153	0.147	0.73	0.48	0.43	0.42	0.41	0.38
t_2		0.68	0.36	0.33	0.25	0.16	0.15	0.81	0.48	0.41	0.37	0.35	0.32	1.7	1.07	0.9	0.84	0.76	0.71
t_3		0.860	0.430	0.340	0.290	0.180	0.160	1.060	0.550	0.440	0.410	0.393	0.360	2.150	1.180	0.920	0.900	0.840	0.837
t_1	CR	43.5	25.5	19.5	16.5	15	13.5	54.01	34.5	26.55	24	22.95	22.05	109.5	72.01	64.51	63.01	61.51	57.01
t_2		51	27	24.75	18.75	12	11.25	60.75	36	30.75	27.75	26.25	24	127.5	80.25	67.5	63	57	53.25
t_3		43	21.50	17.00	14.50	9.00	8.00	53.00	27.50	22.00	20.50	19.65	18.00	107.5	59.00	46.00	45.00	42.00	41.85

t_1 = 0.3333 hr, t_2 = 0.6667 hr, t_3 = 1.0000 hr

In Table 2, the weight loss increases with increase temperature but decreases with increase in concentration of the bitter leaves extract. The graphical representation of the inhibition efficiency of the bitter leaves extract as corrosion inhibitor is shown in Figure 1 below.

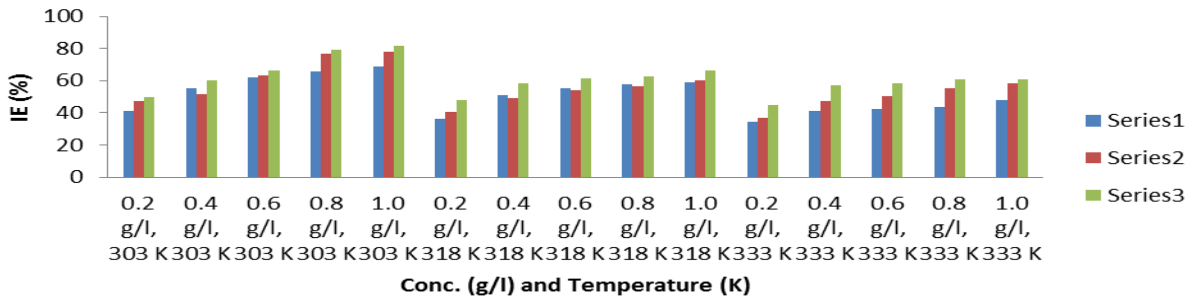

Figure 1, IE versus concentration and temperature at various times; Al in NaOH with bitter leaves extract

The Figure 1 is a graph of inhibition efficiency versus concentration (at various times in series 1, 2, 3). The inhibition efficiency increases with increase in time of immersion. It also increases with increase in concentration of the inhibitor (bitter leaves extract) but decreases with increase in temperature. These observations are in agreement with previous studies [17, 18, 19].

The degree of surface coverage of the Al in the NaOH medium with bitter leaves extract is presented in Tables 3 below. The degree of surface coverage increases with increase in concentration of the bitter leaves extract, but it decreases with increase in temperature.

Table 3, The degree of surface coverage (θ) of Al in NaOH with plants extracts

Inhibitor conc. (g/l)	θ at 303 K	θ at 318 K	θ at 333 K
0.2	0.5000	48.11	45.12
0.4	0.6047	58.49	57.21
0.6	0.6628	61.32	58.14
0.8	0.7907	62.92	60.93
1.0	0.8140	66.04	61.07

3.2.1 The corrosion rate and temperature relationship

The relationships between corrosion rate and temperature for the corrosion inhibition of the Al in NaOH with the bitter leaves extract is presented in Figures 2 below. The Arrhenius equation was used to evaluate the effect of temperature on the rate of corrosion. The Arrhenius equation is expressed by Equation (5) [11, 20].

$$CR = Ae^{-E_a/_{RT}} \quad (7)$$

Where CR is the corrosion rate of the metal, A is the pre-exponential factor, E_a is the activation energy, R is the gas constant. Equation (7) can be linearized to form Equation (8).

$$\ln(CR) = lnA - ({}^{E_a}/_{R})(\tfrac{1}{T}) \quad (8)$$

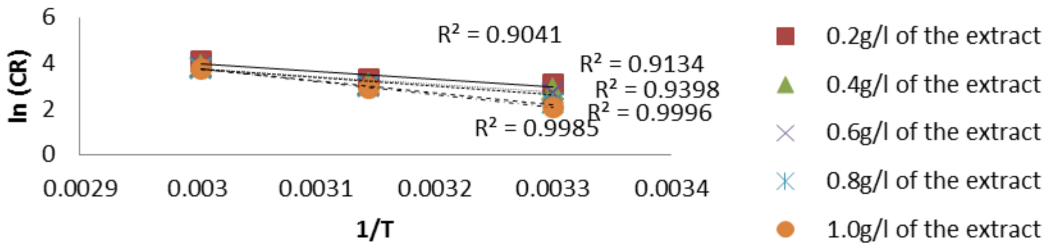

Figure 2, The lnCR (mg/cm^{2}hr) versus 1/T (K^{-1})

In Figure 3, the linear relationships were observed with R^2 close to 1 in all the various concentrations of the bitter leaves extract. The corrosion inhibition process obeys Arrhenius law [20]. Thus, the corrosion rate is temperature dependent.

3.2.2 The activation energy and heat of adsorption for the corrosion inhibition
Considering the corrosion rates of the metal at T_1 and T_2 as CR_1 and CR_2, then Equation (8) can be expressed by Equation (9) [11, 16].

$$\ln\left({}^{CR_2}/_{CR_1}\right) = \left({}^{E_a}/_{2.303R}\right)\left(\frac{1}{T_1} - \frac{1}{T_2}\right) \tag{9}$$

The result of the activation energy for the corrosion inhibition of the Al in the NaOH with bitter leaves extract is presented in Table 4.

Heat of adsorption values for the corrosion inhibition of the Al in the media are presented in Table 4 below. The values of the heat of adsorption Q_{ads} were calculated using Equation (10) below.

$$Q_{ads} = 2.303R\left[\log\left(\frac{\theta_2}{1-\theta_2}\right) - \log\left(\frac{\theta_1}{1-\theta_1}\right)\right] * \frac{T_2.T_1}{T_2-T_1}\ \text{kJmol}^{-1} \tag{10}$$

Where R is the gas constant, θ_1 and θ_2 are the degree of surface coverage at temperatures T_1 and T_2 respectively. As shown in Tables 3, the calculated heat of adsorption values were negative indicating that the adsorption of the extract on the metal surface is exothermic [11].

Table 4, The activation energy and heat of adsorption for the corrosion inhibition of Al in NaOH by various concentrations of bitter leaves extract

Conc. of the plant extract (g/l)	Activation energy, E_a (kJ/mol)	Heat of adsorption, Q_{ads} (kJ/mol)
0.2	65.008	-5.477
0.4	64.103	-3.766
0.6	72.931	-9.712
0.8	99.201	-24.745
1.0	106.555	-28.693

In Tables 4, the values of the heat of adsorption were negative indicating that the adsorption of the extract on the metal surface is exothermic. The result is in agreement with that of previous study [11].

3.2.3 Fitting of Data into Adsorption Isotherm
a. Fitting of data into Langmuir isotherm
Data were fitted into Langmuir isotherm as expressed in Equation (11) [11, 13 14].

$$\frac{C}{\theta} = \frac{1}{K} + C \tag{11}$$

Where C is the concentration of the inhibitor, K is the adsorption equilibrium constant and θ is the degree of surface coverage. In logarithmic form, Equation (11) is expressed as shown in Equation (12).

$$\log\frac{C}{\theta} = \log C - \log K \tag{12}$$

As shown, plot of log(C/ θ) versus log(C) shows linear graphs (Figure 3).

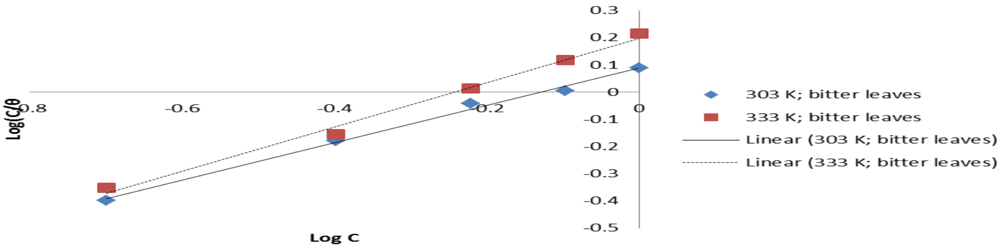

Figure 3, The ln(C/ θ) versus lnC for the corrosion inhibition of Al in NaOH with bitter leaves extract

b. Fitting data into Frumkin isotherm
Data were fitted into Frumkin adsorption isotherm expressed according to Equation (13).

$$\log\left((C)*\left(\frac{\theta}{1-\theta}\right)\right) = 2.303logK + 2\alpha\theta \qquad (13)$$

Where K is the adsorption-desorption constant and α is the lateral interaction term describing the interaction in adsorbed layer. In Figure 5, Plot of log((C)*(θ/(1-θ))) versus θ shows linear graph (Figure 4). The linear relationship shows that Frumkim isotherm was obeyed.

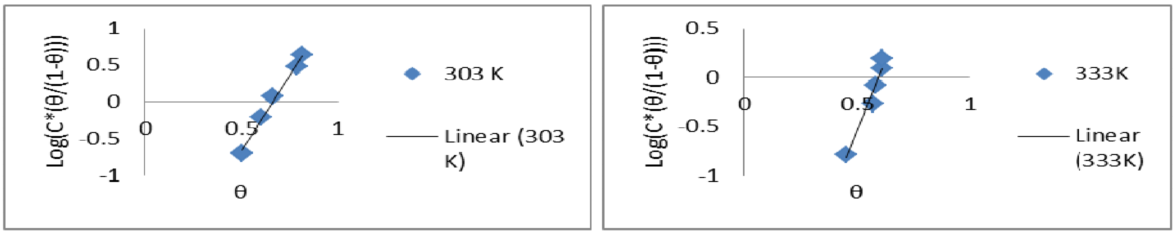

(a) **(b)**
Figure 4, The log(C*(θ/(1-θ))) versus θ for the corrosion inhibition of Al in NaOH by bitter leaves extract; (a) at 303 K, (b) at 333 K

c. Fitting data into Temkin isotherm
Data were fitted into Temkin isotherm as expressed by Equation (14) (Nwabanne and Okafor, 2011).

$$\theta = -\frac{2.303logK}{2a} - \frac{2.303\,logC}{2a} \qquad (14)$$

Where K is the adsorption equilibrium constant, a is the attractive parameter, θ is the degree of surface coverage, C is the concentration of the inhibitor, and K is the adsorption equilibrium constant. In Figure (5), the graph of θ versus logC shows linear relationship indicating that Temkin adsorption isotherm was obeyed.

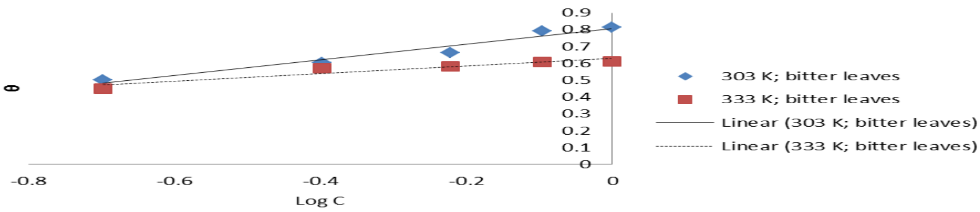

Figure 5, Plot θ versus lnC for the corrosion inhibition of Al in NaOH with the bitter leaf extract

d. Fitting data into Flory-Huggins isotherm
Data were fitted into the Flory-Huggins isotherm as expressed in Equation (15) [11, 12].

$$\log\left(\frac{\theta}{C}\right) = \log K + x\log(1-\theta) \qquad (15)$$

where x is the size parameter and is a measure of the number of adsorbed water molecules substituted by a given inhibitor molecule. Plots of log(θ/C) versus ln(1 - θ) gave linear relationships (Figure 6). The graphs showed that Flory-Huggins isotherm was obeyed.

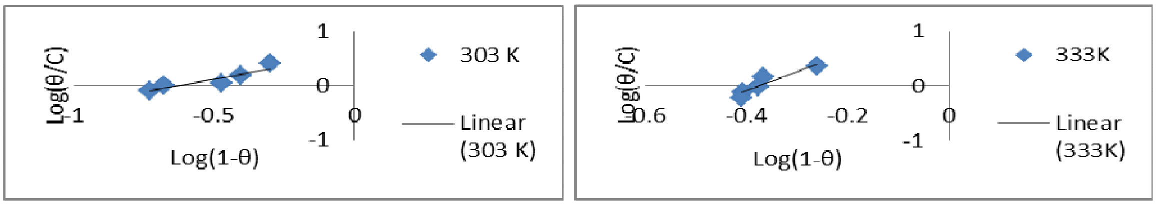

(b) **(b)**

Figure 6, Log(θ/C) versus log(1-θ) for the corrosion inhibition of Al in NaOH by bitter leaves extract; (a) at 303 K, (b) at 333 K

As shown in Figures 3 - 6, the data obtained from the degree of surface coverage were used to test for the applicability of different adsorption isotherms; Langmuir, Frumkin, Temkin and Flory-Huggins isotherms. Linear graphs were observed in all the cases. The degree of determination (correlation coefficient, R^2) is close to one (1). The data were best fitted in the Langmuir isotherm.

3.2.4 The adsorption parameters for the corrosion inhibition

The parameters of the Langmuir, Frumkin, Temkin and Flory-Huggins isotherms are presented in Tables 5. Considering the fitted data to the Langmuir isotherm, the R^2 values are very close to unity, indicating strong adherence to Langmuir adsorption isotherm [15, 16]. The application of Langmuir isotherm to the adsorption of the bitter leaves extract on surface of the Al indicates that there is no interaction between the adsorbate and adsorbent. From the Frumkin adsorption parameters, the lateral interaction term (α) gave positive value suggesting attractive behaviour of the inhibitor on the Al surface [11]. From the Temkin adsorption parameters, the attractive parameter value (a) is negative, indicating that repulsion exists in the adsorption layer [11, 16]. The value of the size parameter (x) is positive. This shows that the adsorbed species of the plant extract is bulky [11]. The free energy of adsorption (ΔG_{ads}) was calculated according to Equation (16) [11, 12].

$$\Delta G_{ads} = -2.303RTlog(55.5K) \quad (16)$$

Where R is the gas constant, T is temperature. The K values obtain from the isotherms (Langmuir, Temkin, Flory-Huggins and Frumkin isotherms) were used to determine the values of ΔG_{ads} according to Equation (16). The values of ΔG_{ads} are presented in Tables 5.

Table 5, Adsorption parameters for the corrosion inhibition process

Adsorption Isotherm	Temperature (k)	R^2	Log K	K	ΔG_{ads} (KJ/mol)	Isotherm property	
Langmuir Isotherm	303	0.9946	-0.0896	0.8136	-9.6		
	333	0.9929	-0.1982	0.6336	-9.9		
Frumkin Isotherm	303	0.9925	-1.1795	0.0661	-3.3	α	2.05556
	333	0.9456	-1.4772	0.0333	-1.7		2.86175
Temkim Isotherm	303	0.953	1.742	55.208	-20.2	a	-2.492
	333	0.894	2.791	618.016	-22.5		-5.118
Flory-Huggins Isotherm	303	0.8502	0.6023	4.009	-13.6	x	0.9611
	333	0.8604	1.2825	19.1646	-19.3		3.4241

In all the cases, the values of ΔG_{ads} are negatives, indicating that adsorption of the plant extract is spontaneous and occurred according to the mechanism of physical adsorption [11, 18].

3.3 Graphical analysis of the inhibition efficiency, IE (%), as determined using RSM

The analysis of inhibition efficiency of the inhibitor is presented in Figure 7.

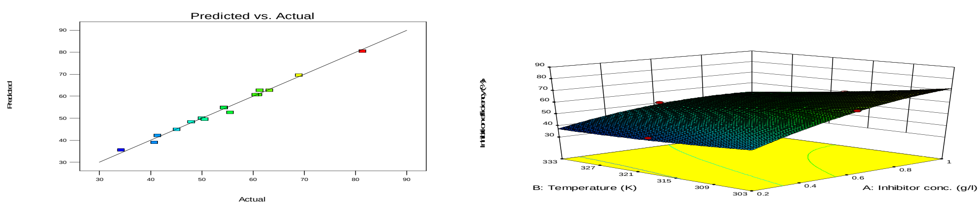

a) **b)**

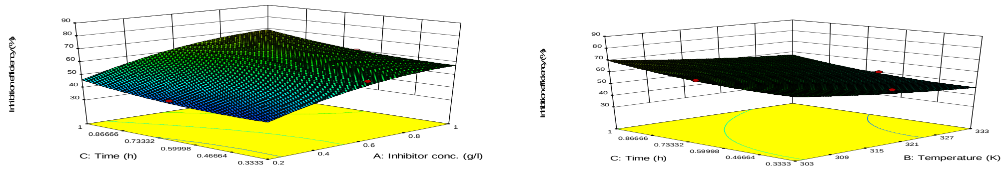

c) **d)**

Figure 7, IE (%) of bitter leaves extract as corrosion inhibitor of Al in NaOH

a) Predicted versus Actual IE (%), b) IE (%) versus inhibitor concentration and temperature c) IE (%) versus inhibitor concentration and time, d) IE (%) versus temperature and time

In Figures 7, the graphical representation of the RSM results is presented. Predicted versus actual plots are used to test the significance of the models order. The predicted versus actual plot shows linear graph. The graphs (3-D surface plots) show the relationship between the factors and responses of the designed experiment. The factors include inhibitor concentration, temperature and time of the Al immersion, while the response is the inhibition efficiency. The result shows that increase in concentration of the inhibitor increases the inhibition efficiency. Also, inhibition efficiency increases with increase in time, but reduces as temperature rises. The ANOVA of the result of the response surface method is shown in Table 6 below.

Table 6, ANOVA for the corrosion inhibition of Al in NaOH by bitter leaves extract

ANOVA for Response Surface Quadratic model; inhibition efficiency						
Analysis of variance table [Partial sum of squares - Type III]						
Source	**Sum of Squares**	**Df**	**Mean Square**	**F Value**	**p-value Prob > F**	
Model	2053.56	9	228.17	111.54	< 0.0001	Significant
A-Inhibitor conc.	*1174.84*	*1*	*1174.84*	*574.33*	*< 0.0001*	
B-Temperature	*435.73*	*1*	*435.73*	*213.01*	*< 0.0001*	
C-Time	*258.06*	*1*	*258.06*	*126.16*	*< 0.0001*	
AB	*107.60*	*1*	*107.60*	*52.60*	*< 0.0001*	
AC	*4.59*	*1*	*4.59*	*2.24*	*0.1650*	
BC	*1.08*	*1*	*1.08*	*0.53*	*0.4840*	
A^2	*68.76*	*1*	*68.76*	*33.61*	*0.0002*	
B^2	*4.64*	*1*	*4.64*	*2.27*	*0.1628*	
C^2	*21.94*	*1*	*21.94*	*10.73*	*0.0084*	
Residual	20.46	10	2.05			
Lack of Fit	*20.46*	*5*	*4.09*			
Pure Error	*0.000*	*5*	*0.000*			
Cor Total	2074.01	19				
Std. Dev.	1.43		R-Squared			0.9901
Mean	54.40		Adj R-Squared			0.9813
C.V. %	2.63		Pred R-Squared			0.9307
PRESS	143.67		Adeq Precision			44.535

3.3.1 Mathematical models of the inhibition efficiency

The mathematical models for inhibition efficiency of the bitter leaves extract as corrosion inhibitor of the Al in the NaOH medium are shown in Equation (17a) for the coded factors and Equation (17b) for the actual factors. The model shows the relationship among the inhibition efficiency (IE), inhibitor concentration (A), temperature (T) and time (C). The model in terms of coded factors predicts the response for given levels of each factor. The coded model shows the relative impact of the factors.

IE = + 54.84 + 10.84A - 6.60B + 5.08C- 3.67A*B+ 0.76A*C+ 0.37BC- 5.00A^2 + 1.30B^2 + C^2 (17a)

IE = +653.70148 +255.19119 * Inhibitor conc. -3.79569 * Temperature -45.43148 * Time -0.61125 * Inhibitor conc. * Temperature +5.68097 * Inhibitor conc. * Time +0.073496 * Temperature * Time -31.25284 * Inhibitor conc.^2 +5.77576E-003 * Temperature^2 +25.41837 * Time^2 (17b)

Considering the significant terms, the models of Equations (21a) ad (21b) reduce to Equations (18a) ad (18b)
IE = + 54.84 + 10.84A - 6.60B + 5.08C- 3.67A*B + 0.76A*C+ 0.37BC- 5.00A^2 + C^2 (18a)

IE = + 653.70148 + 255.19119 * Inhibitor conc. - 3.79569 * Temperature - 45.43148 * Time - 0.61125 * Inhibitor conc. * Temperature - 31.25284 * Inhibitor conc.^2 + 25.41837 * Time^2 (18b)

The Model F-value of 111.54 implies the model is significant. There is only a 0.01% chance that an F-value this large could occur due to noise. Values of "Prob > F" less than 0.0500 indicate model terms are significant. In this case A, B, C, AB, A^2, C^2 are significant model terms. Values greater than 0.1000 indicate the model terms are not significant. The "Pred R-Squared" of 0.9307 is in reasonable agreement with the "Adj R-Squared" of 0.9813; the difference is less than 0.2. "Adeq Precision" measures the signal to noise ratio. A ratio greater than 4 is desirable. The ratio of 44.535 indicates an adequate signal. The graphical representation of the optimum parameters is shown in Figure 8 below.

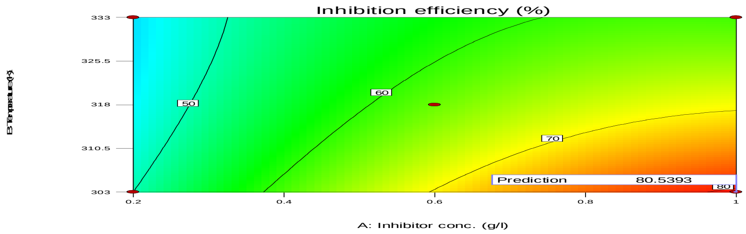

Figure 8, Optimum parameters for the corrosion inhibition process

The optimal conditions for the corrosion inhibition of the Al in NaOH were estimated as concentration of the inhibitor of 1.0 g/l, temperature of 303 K and immersion time of 1hr, under which the optimum inhibition efficiency is 80.54 %.

3.4 The Potentiodynamic Polarization Results

The potentiodynamic polarization curves are presented in Figure 9, below. The plant extract inhibit both cathodic and anodic reactions and acts as mixed-type inhibitor.

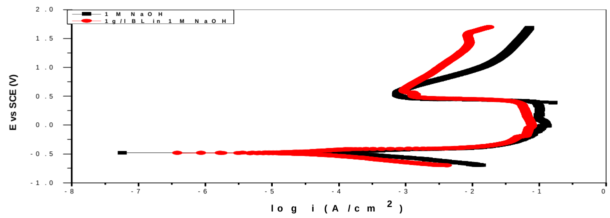

Figure 9, Potentiodynamic polarization curves for Al in NaOH in absence and presence of bitter leaves extract

3.5 FT IR analyses of the bitter leaves extract and corrosion product

The peaks, intensities and assignments (functional groups) of the FT IR analyses of the pure bitter leaves extract (Figure 10) and corrosion products with the bitter leaves extract (Figure 11) are presented in Table 7 below. The spectrum of the graph shows various peaks in the absorbance versus ware length relationship [21, 22]. The analysis of the bitter leaves extract revealed the presence of C=C-H, Ar-H (bend out of plane), C-H (bend in plane), stretched C-O, stretched C=C, stretched C=N, stretched C=O, stretched C≡C, stretched C≡N, stretched C-H and stretched O-H functional groups..

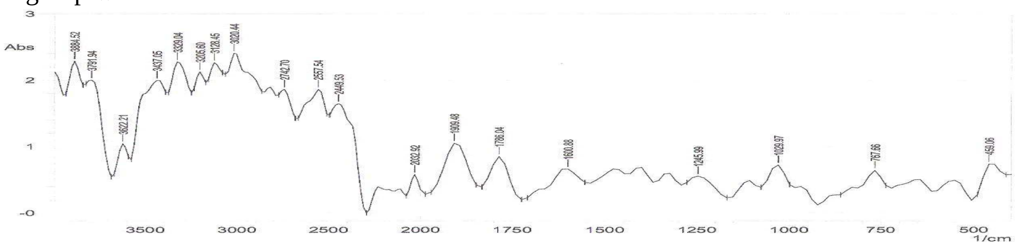

Figure 10, The FT IR spectrum of the bitter leaves extract

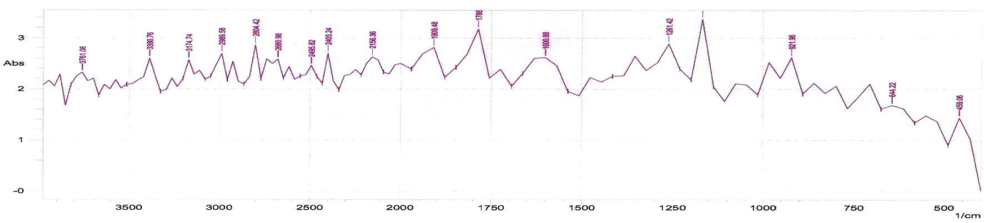

Figure 11, FT IR spectrum of the corrosion product of Al in NaOH with bitter leaf extract

In Table 7, C-H stretched at 3205.6 cm^{-1} peak shifted to 3174.74 cm^{-1}. Also, O-H stretched at 3622.21 cm^{-1} shifted to 3390.76 cm^{-1}. These shifts in peaks in suggest that there is interaction between the Al and some molecules of the inhibitor (bitter leaves extract).

Table 7, Peak, intensity and assignment of FT IR analyses

Bitter leaves extract			Corrosion product of Al in NaOH (containing bitter leaves extract as inhibitor)		
Peak (cm^{-1})	Intensity	Assignment	Peak (cm^{-1})	Intensity	Assignment
767.66	0.6365	C=C-H, Ar-H bend out of plane	644.22	1.6854	C≡C-H, C-H bend
1029.97	0.7209	C-H bend in plane	921.96	2.6189	C=C-H, Ar-H bend out of plane
1245.99	0.5542	C-O stretch	1168.84 1261.42	3.3746 2.8867	C-O stretch
1600.88	0.6621	C=C stretch, C=N stretch	1600.88	2.617	C=C stretch, C=N stretch
1786.04	0.8482	C=O stretch	1786.04	3.1778	C=O stretch
2449.53	1.6445	C≡C stretch, C≡N stretch	2156.36 2403.24	2.6264 2.6979	C≡C stretch, C≡N stretch
2742.70	1.8599	C-H stretch	2804.42	2.8647	C-H stretch
3020.44	2.4052	C-H stretch	2989.58	2.693	C-H stretch
3128.45 3205.60	2.2605 2.1251	C-H stretch	3174.74	2.5713	C-H stretch
3329.04 3437.05 3622.21	2.2743 1.9957 1.0410	O-H stretch,	3390.76	2.6024	O-H stretch

3.6 Metal Surface Study

The micrographs of the corroded metals in the corrosive NaOH in the presence and absence of the inhibitor are presented in Figures.

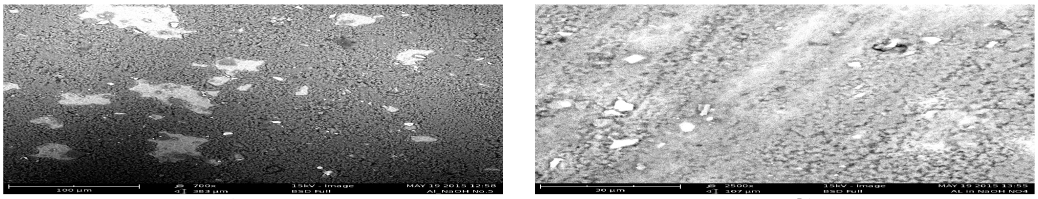

a) b)

Figure 12, The micrograph of corroded Al surface in NaOH.
a) without bitter leaves extract b) with bitter leaves extract.

Figure 12 shows micrographs by SEM of Al specimens exposed in 1M NaOH in the presence and absence of the inhibitor. Considering corroded Al in both media, there were significant differences in the morphologies of the Al surfaces in the presence and absence of the inhibitor. Uniform corrosion was observed. In the absence of the inhibitor, the Al surface was strongly damaged owing to corrosion in the absence of the inhibitor, but in the presence of inhibitor, there is a much smaller damage on the surface. This is attributed to the formation of a good protective film on the Al surface. The surface-nature of the corroded Al in the presence and absence of the inhibitor shows that the bitter leaf extract is a good inhibitor.

CONCLUSION

From the analyses of the experimental results the following conclusions can be made:
1. Adsorption of the extract on the Al surface was spontaneous and occurred according to the mechanism of physical adsorption.
2. The optimal conditions for the corrosion inhibition of the Al in NaOH are concentration of the bitter leaves extract of 1.0 g/l, temperature of 303 K and immersion time of 1hr. The optimum inhibition efficiency of the extract is 80.54 %.
3. The extract of the bitter leaves is a mixed-type inhibitor of Al in NaOH medium.

REFERENCES

[1] Kotz, J. C. and Treichel, P. Chemistry and Chemical Reactivity, 3rd edition, Harcourt Brace Col. Publishers, New York, **1996**.
[2] A. A. El Maghraby, *The Open Corrosion Journal*, 2, **2009**, 189 – 196.
[3] Refat, M. H. and Ishaq, A. Z. Materials 6, **2013**, 2430 – 2451.

[4] K. R. Trethewey and J.Chamberlain, Corrosion for science and Engineering, 2nd Edition, Longman Group Limited, England, **1995**.
[5] P. A. Akah and C. I. Okafor, *Phytother. Res*., 6, **1992**, 171 - 173.
[6] S. C.Masaba, *Ethiopian J. Health Develop*., 13, **2000**, 211 – 216.
[7] H. U. Nwajo, *Nig. J. Physiol. Sci*., 20, **2005**, 39 - 42.
[8] E. M. Mabrouk, H. Shokry and K. M. Abu Al- Naja, *Chem. Met. Alloys*, 4, **2011**, 98-106.
[9] N. O. Eddy, B. I. Ita, S. N. Dodo and E. D. Paul, *Green Chemistry Letters and Reviews*, 5 (1), **2012**, 43 – 53.
[10] N. Nagm, N. G. Kandile, E. A. Badr and M. A. Mohammed, *Corrosion Science* 65, **2012**, 94-103.
[11] L. Octave, Chemical Reaction Engineering, Third Edition, John Wily and Sons, New York, **2003**.
[12] J. T. Nwabanne and V. N. Okafor, *JETEAS*, 2(4), **2011**. 619 - 625.
[13] L. A. Nnanna, I. O. Owate, O. C. Nwadiuko, N. D. Ekekwe and W. J. Oji, *International Journal of Materials and Chemistry*, 3(1), **2013**, 10-16.
[14] X. Li and S. Deng, *Corrosion science* 65, **2012**, 299 - 308.
[15] N. S. Patel, S. Jauhariand, G. N. Mehta, S. S., Al-Deyeb, I. Warad and B. Hammouti, *Int. J. Electrochem. Sc*., 8, **2013**, 2635 – 2655.
[16] I. J. Alinno, and P. M. Ejikeme, *American chemical science journal* 2(4), **2012**, 122 - 135.
[17] B. S. Furniss, A. J. Hannaford, P. W. G. Smith and A. R. Tatchell, Vogel's Textbook of Practical Organic Chemistry, 5th edition, Longman Group, UK, **1989**, 1412-1422.
[18] D. Skoog, D. West, J. Holler and S. Crouch, Fundamentals of Analytical Chemistry, 8th edition, India, **2004**.
[19] E. El Ouariachi, J. Paolini, M. Bouklah, A. Elidrissi, A. Bouyanzer, B. Hammouti, J. M. Desjobert, and J. Costa, *Acta Metal. Sin. (Engl. Lett.)*, 23 (1), **2010**, 13 – 20.
[20] O. M. Ndibe, M. C. Menkiti, M. N. C. Ijomah and O. D. Onukwuli, *EJEAFChe*, 10(9), **2011**, 2847 – 2860.
[21] M. Abdulwahab, A. Kasim, K. A. Bello and J. O. Gaminana, *Advanced Materials Research*, 367, **2012**, 319-325.
[22] V. G. Vasudha, and P. K. Shanmuga, *Research Journal of Chemical Sciences*, 3(1), **2013**, 21 - 26.